Chemical Physics 58 (1981) 325–334
North-Holland Publishing Company

ELECTRONIC EXCITED STATE ENERGY TRANSFER, TRAPPING BY DIMERS AND FLUORESCENCE QUENCHING IN CONCENTRATED DYE SOLUTIONS: PICOSECOND TRANSIENT GRATING EXPERIMENTS

D.R. LUTZ, Keith A. NELSON, C.R. GOCHANOUR and M.D. FAYER
Department of Chemistry, Stanford University, Stanford, California 94305, USA

Received 21 January 1981

Picosecond transient grating experiments are used to examine electronic excited state dynamics in concentrated dye solutions. A model based on radiationless excited state transport and trapping by dimers describes the phenomena responsible for fluorescence quenching. The trapping rate constant is found to have a cubic concentration dependence. Rhodamine 6G dimer lifetimes in glycerol and ethanol are 830 ps and <50 ps respectively. The difference arises due to the viscosity dependence of the dimer radiationless relaxation rate.

1. Introduction

In this paper we examine electronic excited state dynamics in concentrated dye solutions. The experimental evidence suggests that three radiationless processes govern the disposition of electronic excited state energy in this type of system. These three processes are energy transfer between dye molecules [1], trapping by dimers [2], and radiationless relaxation [3] of the dimer excited state. A simple model provides a microscopic dynamical picture of fluorescence quenching [4] in concentrated dye solutions. The results given here relate directly to concentration quenching in dye lasers, an important limiting effect [4]. The basic model also has implications for the construction of luminescent solar concentrators composed of dye solutions in plastic media which have been proposed as a method of augmenting photovoltaic solar energy conversion [5]. In addition, the phenomena under consideration are the important initial steps in photosynthesis, i.e., electronic excitation transfer between chlorophyll chromophors and trapping on reaction centers (dimers) [6].

Qualitatively, the concentration dependent processes which combine and result in fluorescence quenching work in the following manner. At very low concentration, a dye solution absorbs light and fluoresces. At moderate concentrations electronic excited state energy transport occurs due to dipole–dipole interactions between the dye molecules [7]. The energy transport causes fluorescence depolarization effects [1] but does not affect the fluorescence quantum yield. As the concentration is increased further, ground state dimer formation begins [8] and the rate of energy transport continues to increase. By dimers we mean aggregates of two dye molecules which have distinct spectral and other characteristics. Rapid transport among the monomers allows an excitation to find a dimer and become trapped on it. The experiments indicate that back transfer from the excited dimer to monomers is negligible. Once the excitation is trapped on a dimer rapid radiationless relaxation to the ground state occurs, and fluorescence is quenched.

The concentration dependence of the fluorescence quenching is determined by the

0301–0104/81/0000–0000/$02.50

concentration dependence of the trapping. The trapping rate constant depends on both the dimer concentration and the concentration dependent rate of energy transport. The model predicts that the trapping rate constant goes approximately as the cube of the dye concentration. Therefore the onset of fluorescence quenching with increasing concentration is very rapid.

Experimentally, the onset of trapping by dimers manifests itself as an apparent reduction in the excited state lifetime. In the limit that energy transport becomes extremely rapid, the trapping occurs on a time scale short relative to the dimer lifetime, and the excited state population decays with the dimer lifetime. In the two systems studied, rhodamine 6G (R6G) in glycerol and R6G in ethanol, it is determined that the dimer lifetimes are 830 ps and <50 ps respectively. Presumably, the dimers have faster radiationless relaxation rates than the monomers due to the loose nature of the dimer complexes. The dimers undergo rapid configurational changes which enhance the radiationless relaxation rates. This is consistent with the longer dimer lifetime in the glycerol solvent. Since glycerol is much more viscous than ethanol, it will "hold" the dimer complex more rigidly and therefore slow radiationless relaxation.

2. The model

In this section a simple model is presented which describes the dynamics of electronic excited states in concentrated dye solutions. The important features included are excited state energy transport and trapping by dimers. We will utilize a set of rate equations with a trapping rate constant. An exact treatment would involve solution of the master equation for the system in a manner analogous to that used to describe excited state transport in moderate concentration single component dye systems [1]. However, as discussed below, the approach presented here provides a reasonable context in which to analyze the experimental data. The full theoretical treatment using the master equation [9] is necessary for a complete analysis of the experiments.

2.1. The rate equations

In the model the rate equations governing the excited state populations are:

$$dM^*/dt = -K_M M^* - K_T M^*, \tag{1a}$$

$$dD^*/dt = -K_D D^* + K_T M^*. \tag{1b}$$

M^* is the concentration of excited monomers, and D^* is the concentration of excited dimers. K_M is the rate constant for decay of excited monomers to the ground state by radiative and non-radiative processes, and K_D is the analogous rate constant for decay of dimers to the dimer ground state. K_T is the trapping rate constant. The form of the trapping rate constant is described below. The excited monomer population is depleted by decay to the ground state and by trapping. The excited dimer population is depleted by decay and is increased by trapping.

The solutions to eq. (1) are

$$M^* = M_0^* \exp[-(K_M + K_T)t], \tag{2a}$$

$$D^* = [K_T M_0^*/(K_M + K_T - K_D)] \times \{\exp(-K_D t) - \exp[-(K_M + K_T)t]\}. \tag{2b}$$

M_0^* is the initial concentration of excited monomers. For eq. (2b) the initial excited dimer concentration is taken to be zero.

The experimental method used to examine the excited state dynamics is the picosecond transient grating technique [10]. The method will be described in detail in section 3. Here we need to remark that the method produces an excited state spatial fringe pattern and the amplitude of this pattern is measured as a function of time. The signal, $S(t)$, is given by:

$$S(t) = A[OD_p - OD_n]^2. \tag{3}$$

OD_p is the optical density of the sample at the peaks of the fringe pattern, where some of the molecules have been excited. OD_n is the sample optical density at the nulls of the fringe pattern, where there are no excited states. A is a time-

independent constant which involves a number of considerations such as laser beam geometries and is not important for this problem.

The total concentration of absorbing dye species in solution is T, and

$$T = M + D. \tag{4}$$

M is the monomer concentration, and D is the dimer concentration. Since there are no excited states at the fringe nulls,

$$OD_n = \varepsilon l T, \tag{5}$$

where l is the sample length and ε is the extinction coefficient at the wavelength of the probe laser beam. For the experimental systems considered here and for the probe wavelength used, ε is similar for monomers and dimers and for simplicity we will take the monomer and dimer extinction coefficients to be identical. This does not make basic changes in the interpretation of the data presented in section 4. In other situations, a different ε for monomers and dimers can be used. The excited state species do not absorb at the probe wavelength, i.e., there is no excited state to higher lying excited state absorption; therefore

$$OD_p = \varepsilon l (T - M_p^* - D_p^*), \tag{6}$$

where M_p^* and D_p^* are the excited monomer and dimer concentrations of the grating peaks. Substituting eqs. (5) and (6) into eq. (3) gives time-dependent transient grating signal as

$$S(t) = A(\varepsilon l)^2 (M_p^* + D_p^*)^2. \tag{7}$$

Inspection of eq. (7) shows that the time dependence of the signal is determined by the time evolution of the total excited state concentration, $T^*(t)$, where at any point in the crystal

$$T^*(t) = (M^* + D^*). \tag{8}$$

Substituting eqs. (2a) and (2b) into eq. (8) gives:

$$T^*(t) = M_0^* \{\exp[-(K_M + K_T)t] + [K_T/(K_M + K_T - K_D)] \times \{\exp(-K_D t) - \exp[-(K_M + K_T)t]\}\}. \tag{9}$$

$T^*(t)$ is the time-dependent function determined experimentally. It is informative to note some special cases of eq. (9). If K_T is very small, trapping is negligible and $T^*(t)$ decays exponentially with the monomer rate constant, K_M. If $K_D \gg K_M$, K_T then $T^*(t)$ decays exponentially with a rate constant $(K_M + K_T)$. And if $K_T \gg K_M$, K_D excitations are immediately trapped by dimers and $T^*(t)$ decays exponentially with the dimer rate constant, K_D.

2.2. The trapping rate constant

In room temperature systems, excited state energy transport is incoherent [1]. Treatment of single component solutions (no dimers or other traps) by solving the full master equation has demonstrated that, in general, transport is not diffusive in nature [1]. However, at the high concentrations under consideration, transport is non-diffusive only at very short times. Therefore energy transport in these systems is essentially diffusive and isotropic in three dimensions.

In general, trapping is characterized by a time-dependent trapping rate function [11]. Trapping occurs when an excitation has visited enough distinct sites so that on the average it has sampled one trap species. For a random walk on an isotropic three dimensional lattice, the number of distinct sites visited increases linearly with time [12]. Therefore, trapping can be characterized by a trapping rate constant which depends on the site-to-site hopping time. We will assume that trapping can also be characterized by a trapping rate constant in the solution systems discussed here. At high concentration this is reasonable since transport is basically diffusive and isotropic in three dimensions. Although we do not have a periodic lattice, the randomness in spatial distribution of the sites (dye molecules) associated with a solution is taken into consideration in the calculation of the hopping time.

The model we are employing assumes that the site-to-site hopping time is basically unaffected by the presence of the traps. That is, the hopping time can be obtained from the theoretical treatment of the problem of energy transport in solution. This is only reasonable for low trap concentrations. Gochanour et al. [1]

used a diagrammatic self-consistent method to solve the master equation. One of the properties of the system which can be accurately calculated is $G^s(t)$, the time dependent probability of finding the excitation on the site which is excited at $t=0$. A plot of $G^s(t)$ is given in fig. 1 for $C=1$. $G^s(t)$ is obtained by numerically inverting its theoretically calculated Laplace transform. C is the unitless concentration given by [1, 7]:

$$C=\tfrac{4}{3}\pi R_0^3\rho. \tag{10}$$

ρ is the number density and R_0 is the constant which characterizes the strength of the intermolecular transport interaction [7]. The time axis of fig. 1 is in units of t/τ, where τ is the monomer excited state lifetime. $G^s(t)$ scales as C^2, thus $G^s(t)$ can be obtained for any concentration by scaling the time axis of the $C=1$ curve by C^2.

We will define the hopping time h as

$$G^s(h)=1/e, \tag{11}$$

i.e., the hopping time is the time at which the probability of finding the excitation on the initially excited molecule has fallen to $1/e$. For $C=1$, this time is obtained from inspection of fig. 1. Since $G^s(t)$ scales as C^2, the hopping time, h, at any concentration is related to h_1, the hopping time at $C=1$, by

$$h=h_1M_1^2/M^2, \tag{12}$$

where M_1 is the concentration in m/ℓ which gives a unitless concentration $C=1$.

The trapping time, t_T, is the average time for an excitation to find a trap. It is the number of sites which need to be sampled to find a trap multiplied by the time for a step. Then

$$t_T=h/\chi P, \tag{13}$$

where h is the hopping time defined above, and

$$\chi=D/M. \tag{14}$$

$1/\chi$ is the average number of distinct sites (dye molecules) which must be sampled to find a trap (dimer). P is the probability that on any step a distinct site is visited. It corrects for the return to previously visited sites. For an isotropic three

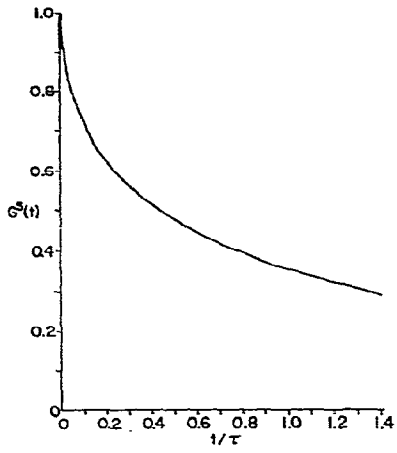

Fig. 1. The time-dependent probability, $G^s(t)$, of finding the excitation on the molecule which is excited at $t=0$ for unitless concentration $C=1$. τ is the excited state lifetime. Curves for all concentrations can be obtained from this curve by appropriate scaling. See text.

dimensional random walk on a lattice, $P=0.7$‡, and we will use this value here. Thus the trapping rate constant is

$$K_T=\chi P/h. \tag{15}$$

The monomer–dimer equilibrium constant q is

$$q=D/M^2, \tag{16}$$

which gives

$$K_T=PqM/h. \tag{17}$$

Substituting eq. (12) into eq. (17) gives the trapping rate constant as

$$K_T=PqM^3/h_1M_1^2, \tag{18}$$

where the concentrations are in m/ℓ. Eq. (18) shows that this model predicts that the trapping rate constant depends on the concentration cubed. Thus trapping increases very rapidly with concentration. This model and the simple cubic concentration dependence of the trapping rate

‡ Our P corresponds to Montroll's $1/u_0$, which is 0.65946 for a simple cubic lattice. This value was misprinted in ref. [12], but the correct value $u_0=1.5164$ was used in later works. See, for example, ref. [13].

constant is reasonably correct only at low dimer concentrations for two reasons. First, the definition of χ in eq. (14) assumes that the monomer concentration M is equal to the total concentration of dye in solution, i.e., that $D \ll M$. Second and fundamental to the problem is the use of $G^s(t)$ from the single component theory to obtain the hopping time in this inherently two component system composed of monomers and traps (dimers). The single component theory properly accounts for "loops" in the transport problem [1]. An excitation leaving an initial molecule (molecule 1) may visit one or more other molecules and then return to molecule 1. All possible paths which return the excitation to molecule 1 (loops) help maintain the probability on molecule 1. Thus the loops slow the decay of $G^s(t)$ and increase the hopping time.

At low trap concentrations, $G^s(t)$ will give an accurate hopping time. However, as the trap concentration increases, some paths that would be loops in a single component system intersect traps which terminate the loops. Thus the return of probability to molecule 1 is reduced, and $G^s(t)$ will decay faster. Thus $G^s(t)$ yields a hopping time which is too long. As the trap concentration becomes large, the hopping time obtained from the single component theory becomes an increasingly poor parameter to use, and it becomes necessary to solve the full master equation to obtain a complete description of the problem [14]. In using the model presented here, there are compensating errors. At the higher dimer concentrations, $G^s(t)$ decays too slowly, but the monomer concentration is overestimated causing the decay of $G^s(t)$ to increase. A comparison with experiment is given in section 4.

In analyzing the data in section 4, R_0 and τ can be determined experimentally for the monomer. These and $G^s(t)$ yield h_1. The concentration of dye in solution is known and in principle the equilibrium constant q can be determined. Therefore K_T can be obtained. This can be used in eq. (9) to calculate the time dependent signal in the transient grating experiment, using K_D obtained at very high concentration. If q is not known, an alternate approach is employed. Transient grating data at a single concentration are used to obtain K_T, then points at other concentrations are calculated by scaling K_T as M^3. This procedure also yields an experimental value for q.

Examination of $T^*(t)$, eq. (9), which gives the time-dependent signal shows that in general the decays are nonexponential. However, in the limiting cases of high and low concentration (very large and very small K_T) the decays are exponential. In between these limits the shapes of the decays are not far from exponential. In the data analysis of section 4 the following procedure is employed. The experimental decays are plotted on logarithmic paper and a decay constant is determined for each concentration. These are then compared to a theoretical effective decay constant, K_{eff}, obtained from eq. (9) by finding the time required for $T^*(t)$ to fall to 1/e. Thus

$$K_{eff} = 1/t^+, \tag{19}$$

with t^+ obtained from eq. (9) by

$$T^*(t^+) = 1/e[T^*(0)]. \tag{20}$$

3. Experimental

The transient grating experiment [10] is illustrated schematically in fig. 2. Two time-coincident laser excitation pulses of wavelength λ cross at an angle θ inside the sample, creating an interference pattern with fringe spacing d given by

$$d = \lambda/2 \sin(\theta/2). \tag{21}$$

Optical absorption results in a spatially varying, sinusoidal excited state concentration distribution. Since the optical properties of the excited states and ground states differ, the periodic excited state concentration distribution acts as a transient grating which Bragg diffracts a variably delayed probe laser pulse incident at the Bragg angle. The grating's diffracting power, defined in eq. (3), decays with time due to excited state relaxation processes. The time

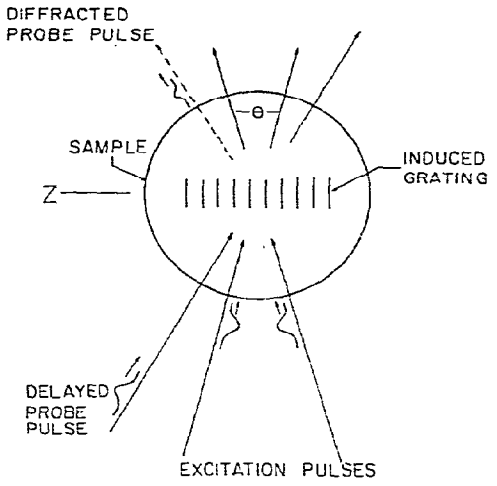

Fig. 2. Schematic illustration of the transient grating experiment. Interference between the incoming excitation pulses results in an oscillatory density of excited states, which Bragg-diffracts the subsequent probe pulse. The diffracted probe is the signal, which reflects the time evolution of the excited state population.

dependence is determined by measurement of the diffracted probe pulse intensity versus probe pulse delay.

Transient grating experiments were used in these measurements for two reasons. First, a TG experiment is inherently more sensitive than a probe pulse experiment although in principle both could provide the same information about the processes under consideration here. In addition the small fringe spacing associated with a TG experiment minimizes problems associated with reabsorption. Second, we found in probe pulse experiments that the highly concentrated samples required very large excitation power densities (small spot sizes) to achieve sufficient bleaching of the ground state population to give reasonable signal. These very high power densities resulted in anomalous power-dependent decays. In a TG experiment large spot sizes can be used so the problem is avoided. As the spot size increases, bleaching is decreased. However, this is offset by an increase in grating volume and therefore the grating diffraction efficiency remains unchanged.

The transient grating experimental setup is illustrated in fig. 3. The laser is a continuously pumped Nd:YAG system which is acousto-optically Q-switched and mode-locked to

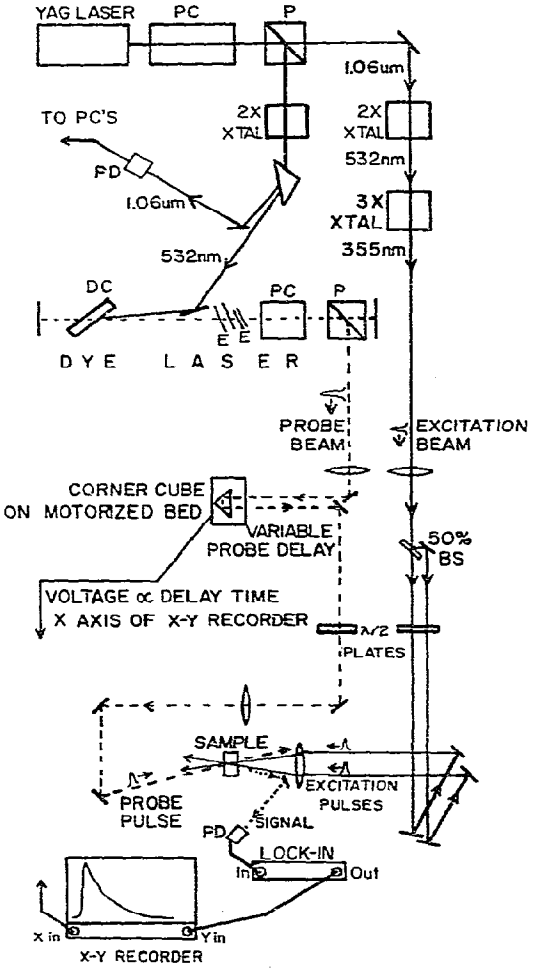

Fig. 3. Transient grating experimental setup. A single 1.06 μm pulse is selected from the YAG mode-locked pulse train, frequency tripled to 355 nm, then split into two excitation pulses. These excitation pulses are then recombined at the sample, creating the transient grating. The remainder of the pulse train is frequency doubled to synchronously pump a tunable dye laser whose output probes the grating after a variable delay. The Bragg-diffracted part of the probe pulse is the transient grating signal. PC≡Pockels cell; P≡polarizer; PD≡photodiode; DC≡dye cell; E≡etalon; BS≡beamsplitter.

produce trains of about 40 pulses at 1.06 μm with 1.3 mJ per pulse train. A single pulse is selected by a Pockels cell with an avalanche transistor driver and frequency tripled to yield a 5 μJ, 50 ps pulse at 355 nm. This is split into the two excitation pulses which are recombined at the sample. The rest of the YAG pulse train is separated by a reflecting polarizer, frequency doubled, and used to synchronously pump a dye laser which is spectrally narrowed and tuned by two intracavity etalons. The dye laser is cavity dumped using another Pockels cell with avalanche transistor driver to give an 8 μJ, 30 ps pulse with a spectral width of 1 cm^{-1}. Both Pockels cells are triggered optically by the IR pulse train to fix the timing between them. The variably delayed dye laser pulse probes the grating at the Bragg angle. The probe pulse is polarized at the magic angle. This eliminates time-dependent depolarization effects from the measurements [1]. The diffracted intensity, measured with a PIN photodiode and lock-in amplifier, is the signal.

The samples were solutions of laser grade rhodamine 6G (New England Nuclear) dissolved in spectro grade ethanol or glycerol. The solutions were mounted in a rotating cell to avoid heating effects. The cell consisted of two glass plates separated by spacers. For the most concentrated solutions the spacers were 5 μm; for the most dilute solutions the spacers were 200 μm.

4. Results and discussion

Transient grating experiments were performed on a series of solutions of rhodamine 6G in glycerol ranging in concentration from 8.7×10^{-4} to 0.05 m/ℓ. A typical result and log plot are shown in fig. 4. In all cases the data appeared to decay exponentially for several lifetimes. Thus the decay could be characterized by an effective rate constant, K_{eff}, as discussed in section 2. Long range energy transport could carry excitations from grating peaks to grating nulls, washing out the grating pattern [15]. This would contribute to the TG signal decay.

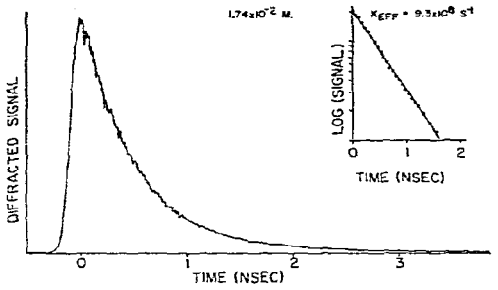

Fig. 4. Transient grating results for rhodamine 6G in glycerol. Probe wavelength = 560 nm. Inset shows the log of the data versus time. The effective decay constant for this dataset is $K_{eff} = 9.3 \times 10^{8}\ s^{-1}$.

However, the time dependence of the signal showed no grating fringe spacing dependence. This demonstrates that destruction of the grating pattern by long range spatial energy transport is not responsible for the observed time dependence.

A plot of K_{eff} versus R6G concentration is shown in fig. 5. First consider the qualitative features of the concentration dependence. At low concentration, K_{eff} is concentration independent and given by the monomer decay rate: $K_{eff} = K_M = 3.3 \times 10^{-8}\ s^{-1}$. This represents

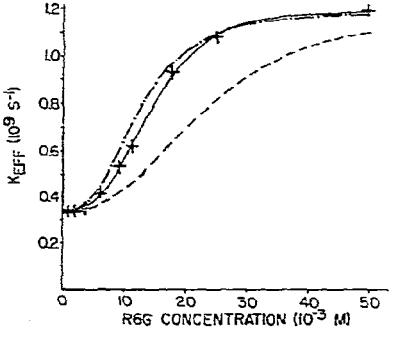

Fig. 5. Effective decay constant, K_{eff}, versus concentration of rhodamine 6G in glycerol. + indicates experimental data. As the R6G concentration increases, excited state transport and trapping by R6G dimers becomes increasingly rapid. Fast radiationless relaxation by the dimers decreases the excited state lifetime and quenches fluorescence. The solid curve is calculated using the results of section 2. The other curves are described in section 4.

the limit $K_T = 0$, i.e., no trapping, since there are few dimers and transport is relatively slow. At high concentration, K_{eff} is essentially concentration independent and given by the dimer decay rate: $K_{eff} \approx K_D = 1.2 \times 10^9\ s^{-1}$ and the dimer lifetime is 830 ps. This corresponds to the limiting case $K_T \gg K_D, K_M$ (instantaneous trapping) which occurs at high concentration since the dimer population is substantial and energy transfer, characterized by the hopping time h, is fast. The observed concentration dependence also verifies the assumption that dimer–monomer back transfer is negligible. Significant back transfer would result in a shortening of the lifetime proportional only to the time spent on dimers and would result in a much slower change in the observed lifetime with increasing concentration. The absence of back transfer is presumably due to significant structural relaxation (excimer-like) by the dimer upon excitation. Between the two concentration limits, K_{eff} varies sharply with concentration due to the M^3 concentration dependence of K_T [see eq. (18)].

In addition to affecting excited state dynamical processes dimer formation should give rise to changes in the ground state absorption spectra of the solutions. Fig. 6 shows absorption spectra of low and high concentration solutions. The spectra are different, especially in the region around 500 nm. Spectra of solutions of many concentrations were examined, and it was found that the onset of spectral changes coincides with the onset of changes in the excited state decay rate. This clearly demonstrates that the concentration dependence of the decay rate is due to changes in the ground state molecules and not to processes such as excimer formation which only affect the excited states.

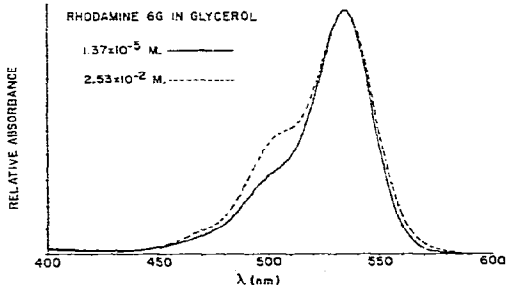

Fig. 6. Absorption spectra of R6G in glycerol at low and high concentrations. The spectra have been normalized to the same maximum height. The change in the shape of the spectra is due to dimer formation at high concentrations.

Detailed comparison of the model and the experimental data is given in fig. 5. The data were analyzed as discussed in section 2.2. The monomer and dimer decay rates were determined from the TG data at low and high concentration respectively. Since the equilibrium constant, q, is not known, TG data at a single intermediate concentration were used to determine K_T. Decay constants K_{eff} were then calculated at other concentrations by scaling K_T as the concentration cubed and using eq. (9). The calculated values of K_{eff} as a function of concentration yielded the curve (solid line) shown in fig. 5. The curve fits the experimentally measured decay constants over the range of concentrations, indicating that the microscopic model is basically correct.

Knowing K_T allows calculation of the equilibrium constant for dimer formation from eq. (18). The hopping time, h_1, can be calculated using the result $R_0 = 50$ Å determined by picosecond fluorescence depolarization measurements [1] and by spectroscopic measurements [16]. Eq. (10) then gives $M_1 = 3.17 \times 10^{-3}\ m/\ell$ corresponding to the unitless concentration $C = 1$. From fig. 1, the hopping time is $h_1 = 0.90\tau = 2.70$ ns. Finally $K_T = 1.62 \times 10^7\ s^{-1}$ at this concentration. This yields an equilibrium constant $q = 9.7\ \ell/m$. Equilibrium constants for various solutions of R6G in glycerol–water mixtures have been determined from concentration dependent absorption spectra to range from 28 ℓ/m in the solution with the most water to 11 ℓ/m in the solution with the least water [8b]. The equilibrium constant which resulted from the time-dependent measurements is consistent with these values. This provides additional support for the basic model.

The excellent agreement between the calculated solid line and the data in fig. 5 arises

from a cancellation of errors. As discussed in section 2.2, the single component theory used to obtain $G^s(t)$ yields hopping times which are increasingly too slow as the dimer (trap) concentration increases. This is offset by the model's overestimation of the monomer concentration at high dimer concentrations. Using the same set of parameters employed to calculate the solid line, but now properly handling the monomer concentration, yields the dashed line in fig. 5. As expected it falls below the data. The dashed line demonstrates the extent to which the use of $G^s(t)$ from the single component theory and experiments underestimates the trapping rate. The dot-dash line in fig. 5 was calculated using the correct concentration dependence and increasing the pairwise intermolecular interaction parameter R_0 from the experimentally determined value of 50 Å for the single component system to a value of 65 Å. This causes $G^s(t)$ to decay more rapidly, which increases the trapping rate. However, this procedure affects $G^s(t)$ at all concentrations while in a correct theory $G^s(t)$ would only differ from the single component theory at high trap concentrations. Thus the dot-dash curve lies above the experimental data at the lower concentrations.

The net result is that the basic physical model can account for the experimental data. However, a comprehensive description requires the solution of the master equation. The fact that the cubic concentration dependence of the formulation presented in section 2 reproduces the data (solid line in fig. 5) indicates that this dependence should emerge from a full theoretical treatment.

Transient grating experiments were also performed on a series of solutions of R6G in ethanol. The data are marred by an experimental artifact which results from coupling between the crossed laser pulses and the acoustic field of the solvent. This introduces time-dependent oscillations into the TG data. This phenomenon has been observed in other materials and is discussed in detail elsewhere [17]. It does not occur in glycerol, presumably because of unusually large acoustic damping effects.

Approximate decay rate constants were estimated from the TG data and these are plotted versus concentration in fig. 7. These data must be considered qualitative in nature. At low concentration the rate constant is determined by the monomer decay rate: $K_{\text{eff}} = K_M = 2.7 \times 10^8\ \text{s}^{-1}$. As the concentration rises, the decay rate rapidly increases. The measurement at the highest concentration is instrumentally limited by the laser pulse duration. The excited state decay constant at high concentration is at least $2 \times 10^{10}\ \text{s}^{-1}$, i.e., the lifetime is less than 50 ps. This is in marked contrast to the glycerol solutions, in which the dimer lifetime is 830 ps.

Clearly the radiationless relaxation rates of the loosely bound dimer are influenced by the solvent viscosity. The low viscosity of ethanol permits rapid configurational fluctuations which lead to very fast radiationless relaxation. The fluctuations occur more slowly in glycerol, and thus the dimer lifetime is longer.

5. Concluding remarks

The two major results of this paper are as follows. First, a microscopic physical model of excited state dynamics in dye solutions involving concentration-dependent trapping has been presented and compared to experiment. Second, the R6G dimer lifetime is more than an order of magnitude shorter in ethanol than in glycerol.

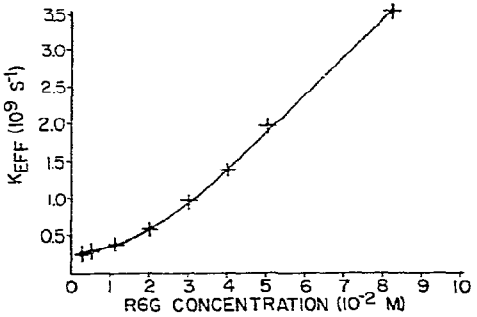

Fig. 7. Effective decay constant, K_{eff}, versus concentration of rhodamine 6G in ethanol. + indicates experimentally determined points. These data are qualitative due to an experimental artifact. See text.

This suggests that the radiationless relaxation rates of the loosely bound dimer complexes are strongly influenced by the viscosity of the medium.

These results directly apply to concentration-dependent fluorescence quenching in dye solutions. Trapping on dimers, which increases as the cube of the dye concentration, leads to fast radiationless relaxation and thus quenches fluorescence. The solvent-dependent dimer lifetime also influences fluorescence quenching. In high concentration R6G in ethanol solutions, fluorescence is completely quenched since the dimer radiationless relaxation rate is extremely fast. In high concentration glycerol solutions, fluorescence is only partially quenched since the dimer decay rate is only four times faster than the monomer decay rate. This allows some radiative relaxation to occur.

The description of excited state dynamics in concentrated dye solutions also has implications for the design of dye solution luminescent solar concentrators for photovoltaic devices. Fluorescence quenching due to dimers may place a limit on the dye concentration which can be used in the solar collector. This limit will depend on the medium. In more viscous or rigid media, fluorescence quenching is reduced. Also, different materials will have different monomer–dimer equilibrium constants. It could be necessary to use polymeric materials in which the chromophors are attached to the polymers in a manner that inhibits dimer formation. We are currently pursuing additional experimental and theoretical projects on both single component and multicomponent concentrated dye systems to extend our understanding of the important radiative and nonradiative phenomena in these materials and to examine questions pertaining to their applications.

Acknowledgement

This work was supported by the Department of Energy, Division of Materials Research: Contract # DE-AT03-79ER 10467.

References

[1] C.R. Gochanour, H.C. Andersen and M.D. Fayer, J. Chem. Phys. 70 (1979) 4254;
C.R. Gochanour and M.D. Fayer, J. Phys. Chem. (1981), to be published.
[2] G.F. Imbusch, Phys. Rev. 153 (1967) 326.
[3] J.B. Birks, Photophysics of aromatic molecules (Wiley–Interscience, New York, 1970) pp. 142–192.
[4] F.P. Schäfer, in: Topics in Applied Physics, Vol. 1, 2nd revised Ed. (Springer, Berlin, 1977) pp. 21–24; 158–160.
[5] W.H. Weber and J. Lambe, Appl. Opt. 15 (1976) 2299;
J.S. Batchelder, A.H. Zewail and T. Cole, Appl. Opt. 18 (1979) 3090.
[6] I. Berlman, Energy transfer parameters of aromatic compounds, (Academic Press, New York, 1973) p. 62;
J.D. McElroy, G. Feher, and D.C. Mauzerall, Biochim. Biophys. Acta 267 (1972) 363;
J.R. Norris, M.E. Druyan and J.J. Katz, J. Am. Chem. Soc. 95 (1973) 1680.
[7] I. Berlman, Energy transfer parameters of aromatic compounds (Academic Press, New York, 1973) pp. 27–47, and references therein.
[8] (a) J.E. Selwyn and J.I. Steinfeld, J. Phys. Chem. 76 (1972) 762;
(b) C. Bojarski, J. Kuśba and G. Obermueller, Acta Phys. Polon. A48 (1975) 85.
[9] D.L. Huber, Phys. Rev. B: Condens. Matter 20 (1979) 2307, 5333.
[10] H.J. Eichler, Opt. Acta 24 (1977) 631;
A. von Jena and H.E. Lessing, Opt. Quant. Elect. 11 (1979) 419.
[11] R.D. Wieting, M.D. Fayer and D.D. Dlott, J. Chem. Phys. 69 (1978) 1996.
[12] E. W. Montroll, in: Proceedings of the Symposium on Applied Mathematics, Vol. 16 (Am. Math. Soc., Providence, 1964) p. 193 (see also eq. (1c), p. 210).
[13] E.W. Montroll, J. Math. Phys. 6 (1965) 167.
[14] R.F. Loring, L. Madison, R.J.D. Miller, H.C. Andersen and M.D. Fayer, to be published.
[15] J.R. Salcedo, A.E. Siegman, D.D. Dlott and M.D. Fayer, Phys. Rev. Letters 41 (1978) 131;
M.D. Fayer, in: Modern problems in solid state physics: Molecular solids, ed. R.M. Hochstrasser (North-Holland, Amsterdam, 1981, to be published).
[16] M.D. Ediger, R.S. Moog and M.D. Fayer, to be published.
[17] K.A. Nelson, D.R. Lutz, L. Madison and M.D. Fayer, Phys. Rev. B(1981), to be published;
K.A. Nelson and M.D. Fayer, J. Chem. Phys. 72 (1980) 5202.